Available online: http://journal.uir.ac.id/index.php/JEEE/index

Journal of Earth Energy Engineering

Publisher: Universitas Islam Riau (UIR) Press

Identification of Reservoir Distribution Using Extended Elastic Impedance (EEI) Inversion in the "Z" Field of the Kutai Basin

Zikra Miftahul Haq*[1], Eki Komara[1], Wien Lestari[1]
[1]Geophysical Engineering Department, Institut Teknologi Sepuluh Nopember, Surabaya, Indonesia
*Corresponding Author: zikramiftahul.h@gmail.com

Article History:

Received: May 20, 2023
Receive in Revised Form: May 31, 2023
Accepted: June 10, 2023

Keywords:

Chi Angle, Extended Elastic Impedance, Inversion, Kutai Basin, Reservoir Distribution.

Abstract

This research was conducted using EEI inversion on seismic data in Z Field, Kutai Basin. The EEI inversion is effectively used to determine the reservoir distribution by eliminating the angle limit on the elastic impedance to the Chi angle so that it can be correlated with petrophysical parameters that are sensitive to lithology and fluids. The data used in this study are well data, checkshots, horizons, and partial-stack angle gather 3D seismic data. The data obtained is processed to obtain the target zone first based on log interpretation. Based on data processing, the target zone is obtained at 1513 m to 1531 m. Sensitivity analysis was conducted to determine the sensitive parameters, which can separate the lithology of the formation. In the sensitivity analysis, the most sensitive log to separate lithology is the Vp/VS log, which can separate sandstone, shale, and coal. Furthermore, the EEI inversion analysis was carried out to obtain the most suiTable model for the inversion, the Based Hard Constraint model was obtained with a correlation reaching 0.997 and an error value of 0.078. Based on the EEI inversion, the target zone in the Z-field at a depth of 1258 ms - 1269 ms with a sandstone reservoir in the EEI range of 6000 (m/s)(g/cc) - 7500 (m/s)(g/cc) which spreads from northeast to south. The distribution of the sandstone reservoir is surrounded by coal with a range of EEI 7500 (m/s)(g/cc) - 12000 (m/s)(g/cc), and also the distribution of shale in the EEI range of 7500(m/s)(g/cc) - 9200(m/s)(g/cc).

INTRODUCTION

The Kutai Basin in East Kalimantan, Indonesia, is renowned for being a vast and highly productive oil and gas basin. It holds substantial oil and gas reserves within its Miocene delta system (Moss., 2018). With an impressive track record, this hydrocarbon basin has already yielded the discovery of approximately 14 billion barrels of oil (Nugrahanto et al., 2021). Spanning an area of 165,000 square kilometers, the Kutai Basin stands as one of the largest and deepest basins in Indonesia, encompassing Tertiary deposits that reach depths of up to 12,000 meters (Alam et al., 1998).

The deepest Tertiary basin in Indonesia is the Kutai Basin, which has accumulated an impressive sediment thickness of over 14 kilometers. This basin is bordered by various geological features, including the Paternoster platform, Barito Basin, and Meratus Mountains to the south, the Schwaner Block to the southwest, the Mangkalihat plateau to the north-northeast, and the Central Kalimantan Mountains to the west and north (Moss and Chambers, 1999). The Kutai Basin itself is further divided into two distinct sections: the Upper Kutai Basin, characterized by Paleogene outcrops and Cenozoic volcanics displaying a pronounced northwest-southeast trending structure, and the Lower Kutai Basin, where Miocene strata are exposed and exhibit a north-northeast trending structure (McClay et al., 2000).

The Kutai Basin's configuration is primarily characterized by a sequence of folds oriented in a NNE ± SSW direction, alongside supplementary faults that run parallel to the curved and parallel coastline referred to as the Samarinda Anticlinorium. These geological features played a significant role in the formation of productive reservoirs within the basin (Satyana et al., 1999).

DOI: 10.25299/jeee.2023.13955
eISSN: 2540-9352 pISSN: 2301-8097

Presently, researchers are actively engaged in further exploration and development of the existing fields in this basin. Based ona scientific standpoint, the optimal approach for identifying oil and gas reservoirs involves understanding and interpreting physical parameters that indicate the presence of hydrocarbons and the geological structure. The effectiveness of the EEI method in this regard positions it as one of the foremost techniques for addressing contemporary exploration challenges (Pranata et al., 2017).

In many instances, inversion techniques enhance the resolution of traditional seismic methods and elevate the analysis of reservoir parameters to a higher level (Veeken and da Silva, 2004). Seismic inversion serves as a means to integrate well log and seismic data, with the objective of translating seismic information into the rock and fluid properties of the subsurface (Purnomo et al., 2023). Within quantitative seismic interpretation, seismic inversion stands out as one of the most powerful tools for predicting pore fluid content, reservoir lithology, and properties in regions where well control data is limited (Aleboiuyeh and Chehrazi, 2018).

Multiple studies have demonstrated the effectiveness of EEI as a technique for reservoir characterization. Researchers have successfully utilized EEI inversion to delineate contrasts between reservoir and non-reservoir regions, enabling the identification of hydrocarbon-rich areas (Ali et al., 2021). Moreover, the drilling outcomes align with the rock brittleness index forecasted by the EEI inversion, affirming the reliability and accuracy of utilizing EEI inversion outcomes to predict the distribution of rock brittleness index (Sun et al., 2021).

The relationship between EEI logs and petrophysical properties of interest is direct, allowing for direct acquisition of seismic EEI reflectivity volumes from prestack data through linear projection in sin2theta. This directness is a key advantage of the EEI method, eliminating the need for intermediate steps such as analyzing conventional AVO attributes like intercepts and gradients (Hicks and Francis, 2006). The theoretical foundation of the EEI method is rooted in the AVO (Amplitude Variation with Offset) theory (Sun et al., 2021). EEI is a refinement of the EI introduced by Whitcombe in 2002, Elastic Impedance (EI) is a function of P-wave velocity (VP), S-wave velocity (Vs), density (ρ) and angle of incidence (θ) (Connolly, 1999). EEI removing its dimension dependence on angles, which is a new function called (Chi angle or project angle) which varies between -90° and +90°. (Whitcombe et al., 2002).

EEI uses the concept of coordinate rotation in the acoustic impedances (AI) and gradient impedances (GI) domains to relate rock elastic parameters to seismic reflectivity, with non-zero incident angle (Whitcombe et al. 2002). In the EEI equation, changes are made by replacing sin2 with tan χ so that the equation is defined between ±∞. In the EEI concept, the reflectivity is also scaled to normal reflectivity by multiplying it by cos, so that the reflectivity does not exceed unity. In the Zeoppritz equation, a substitution is made, thus, equation (1) becomes :

$$R = A + B \tan^2\chi \qquad (1)$$

$$R = \frac{(A\cos\chi + B\sin\chi)}{\cos\chi} \qquad (2)$$

So for the extended elastic impedance equation, we get equation (3):

$$EEI(\chi) = \alpha_o\rho_o\left[\left(\frac{\alpha}{\alpha_o}\right)^p\left(\frac{\beta}{\beta_o}\right)^q\left(\frac{\rho}{\rho_o}\right)^r\right] \qquad (3)$$

Where :

$p = (\cos\chi + \sin\chi)$

$q = -8K\sin\chi$

$r = (\cos\chi - 4K\sin\chi)$

The following is an example of the EEI response in a case study with various variations of the Chi angle (Figure 1).

Journal of Earth Energy Engineering
Vol. 12 No. 2s 2023: IC-UPERTAIN 2022, pp 1-10

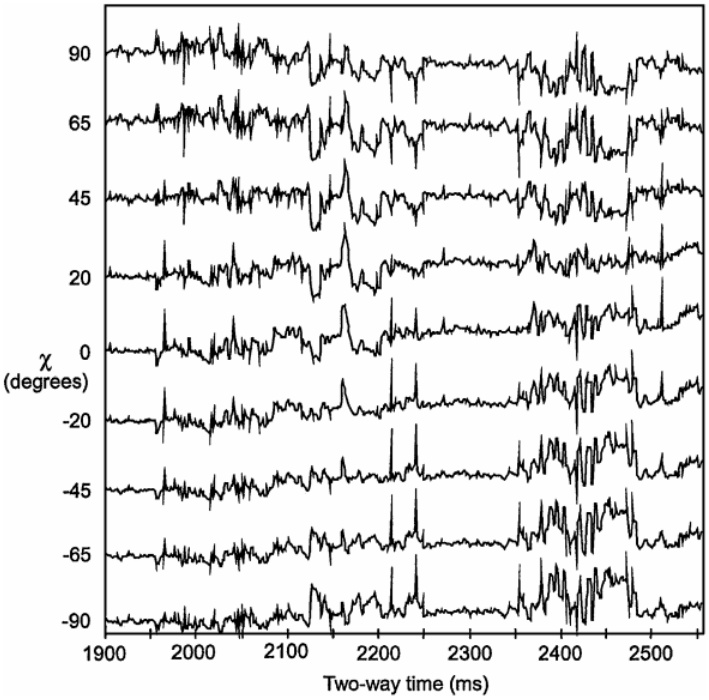

Figure 1. Examples of EEI responses with various variations of the angleχ (Whitcombe, 2002)

MATERIAL AND METHODS

Data

In this study, there are some data needed, including seismic data, well-logs, checkshots, and horizons.

Seismic data

The seismic data used in this study is the 3D Partial Angle Stack seismic data which consists ofnear angle stack data (2º-12º), mid angle stack data (10º-22º), dan far angle stack data (20º-32º).

Table 1. Description of seismic data

No	Parameters	Description
1	Inline Count	752 (1999-2750)
2	Crossline Count	508 (8900-9407)
3	Sampling Rate	2 ms
4	Polarity Type	SEG Normal
5	Wavelet Type	Zero Phase

Well Data

The well data used in this study is WELL-Z which is located in Field Z, Kutai Basinin. LAS format which consistsof: Gamma-ray, resistivity, neutron porosity, density, water saturation, effective porosity, p-wave, and s- waves.

Checkshots Data

In this study, checkshot data is used to help position the well in its actual position by correlating with the P-wave log, so that the two-way time (twt) on the synthetic seismogram will be the same as the seismic data two-way time (twt). The checkshot data used is 66 for each TVDSD and TWT.

Copyright @ Haq et al; This work is licensed under a Creative Commons Attribution-ShareAlike 4.0 International License.

Horizons Data

A horizon is a boundary (marker) laterally on seismic data on a structure or layer boundary that is used to facilitate the interpretation of seismic data. In this study, 4 data horizons were used to assist in the interpretation of seismic data.

Data processing

In this study, data processing was carried out using Hampson-Russell software. This software analyzes well-log, well-seismic-tie data, up to the seismic inversion stage using EEI. The following is a flow chart from this study which is shown in the Figure.

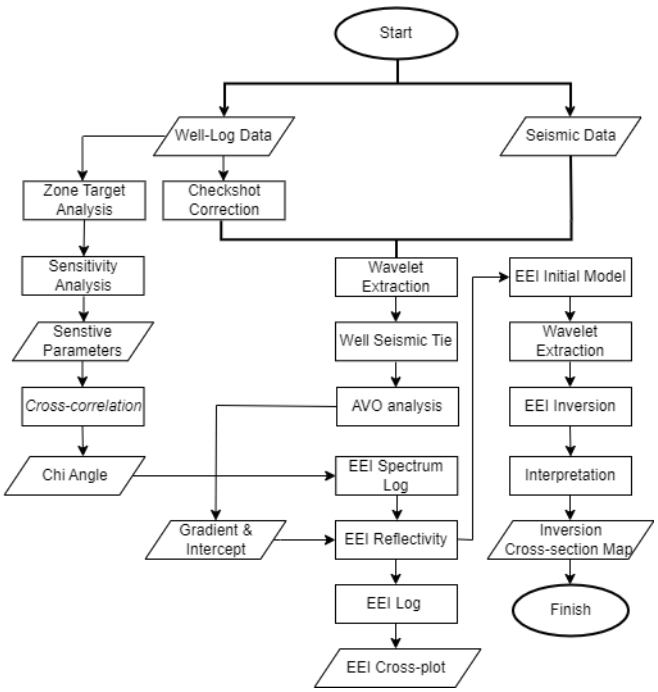

Figure 2. The Workflow of EEI Inversion

RESULTS AND DISCUSSION

Chi Angle Analysis

Chi angle analysis is carried out to determine the right Chi angle value to be used for the EEI inversion process later. The determination of the Chi angle is carried out by cross-correlation between the cross-correlation coefficients and the log attribute in the predetermined target zone. In this process, settings are made on several parameters that will be used, such as the K value and the domain parameters on the target. In this study, the correlation was carried out for all available log data, using the K parameter calculated based on log data. Based on the correlation results, it was found that Vp/Vs was the most sensitive attribute (Figure 3), with a correlation value of 0.997629 with a Chi angle of 38 degrees (Figure 4).

Journal of Earth Energy Engineering
Vol. 12 No. 2s 2023: IC-UPERTAIN 2022, pp 1-10

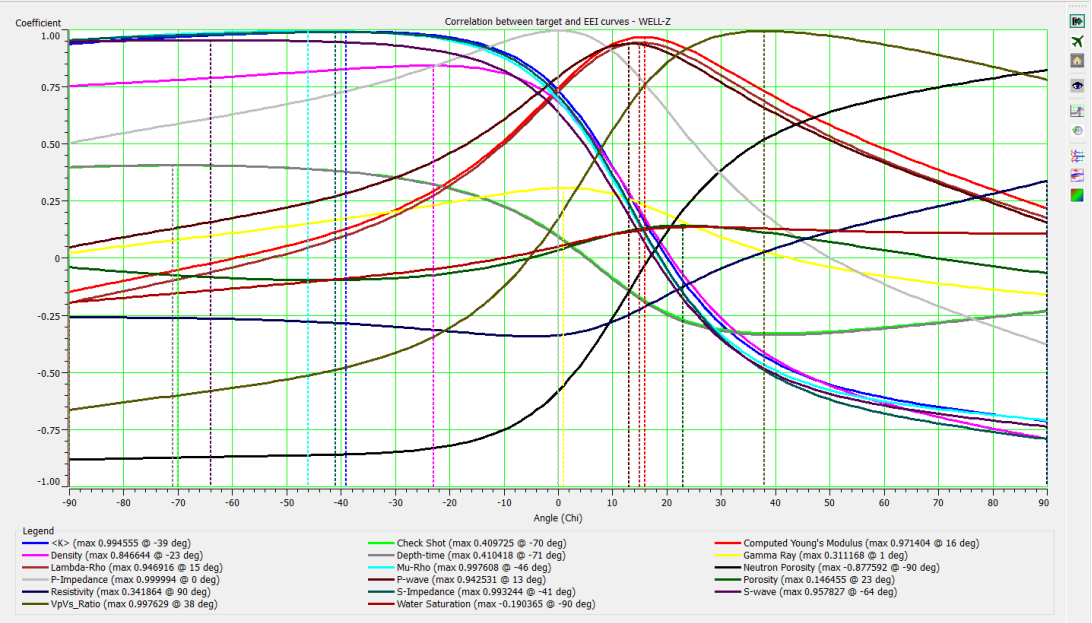

Figure 3. Chi angle cross-correlation

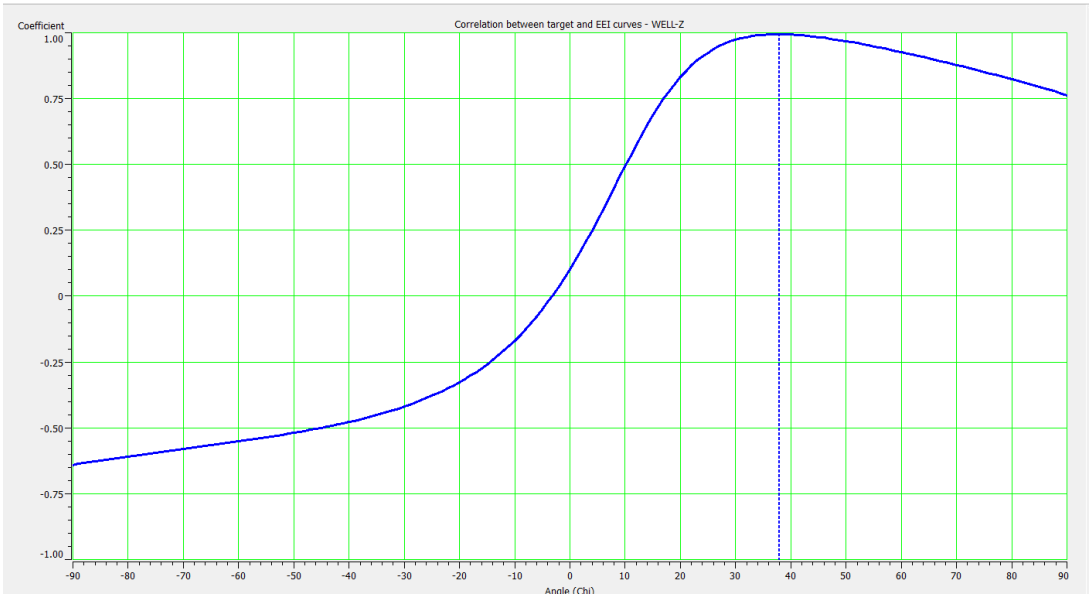

Figure 4. Cross-correlation of Chi *38º* angle withVp/Vs

EEI Sensitivity Analysis

EEI sensitivity analysis was carried out to ensure that the EEI logs that have been made can separate lithology and hydrocarbon zones. Sensitivity analysis was carried out by carrying out the EEI and gamma-ray log crossplots with PHIE and SW color keys. In Figure 5, a cross-plot is carried out between the EEI log and gamma-ray using the PHIE color key (effective porosity). In Figure 5 it can be seen that this cross-plot can separate sandstone, shale (shale), and coal. The EEI log cut-off value on the X-axis for the coal and sandstone seams is 7500(m/s)*(g/cc). Seams with coal distribution are in the EEI 7500(m/s)(g/cc) -12000 (m/s)(g/cc) range marked by cream shading (Figure 5), sandstone layers are in the EEI 6000 (m /s)(g/cc) -7500(m/s)(g/cc) is characterized by red shading (Figure 5), and the shale layer is in the EEI range 7500-9200(m/s)(g /cc) is indicated by blue shading (Figure 5). The EEI log cut-off value on the Y-axis is 90 API. Seams filled with coal and sandstone are in the low gamma-ray range of 40-90 API. As for the shale layer, there is a range of 90-160 API.

Copyright @ Haq et al; This work is licensed under a Creative Commons Attribution-ShareAlike 4.0 International License.

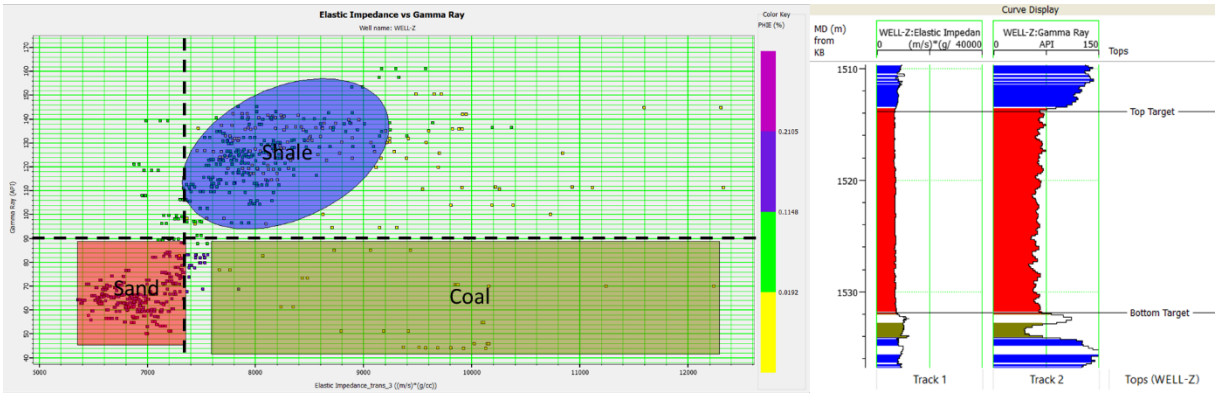

Figure 5. Cross-plot of EEI 38º and Gamma-ray logs, with PHIE color key

In Figure 6, a cross-plot is carried out between the EEI log and gamma-ray using the SW (saturation water) color key. In Figure 6 it can be seen that this cross-plot can separate the HC, brine, and coal zones. The cut-off value of the EEI log on the X-axis for the coal seams and the hydrocarbon zone is 7500 (m/s)*(g/cc). Seams with coal distribution are in the EEI range of 7500(m/s)(g/cc) - 12000 (m/s)(g/cc) characterized by cream shading (Figure 6), sandstone layers (HC zone) are in the range The EEI is in the range of 6000(m/s)(g/cc) - 7500(m/s)(g/cc) indicated by red shading (Figure 8), and the brine zone is in the EEI range of 6000(m/s)(g /cc) - 10000(m/s)(g/cc) indicated by blue shading (Figure 8). The EEI log cut-off value on the Y-axis is 90 API. Seams with coal and HC zones are in low gamma-ray in the range of 40-90 API. As for the brine zone, there is a range of 92-150 API. In the data distribution, it can also be seen that the HC zone is in the yellow color key, which means it has a small SW of 0.7, while the brine and coal zones are red. This indicates that the HC zone has a relatively small SW, namely <0.7 which indicates that this zone contains little water, which is suspected to be filled with gas.

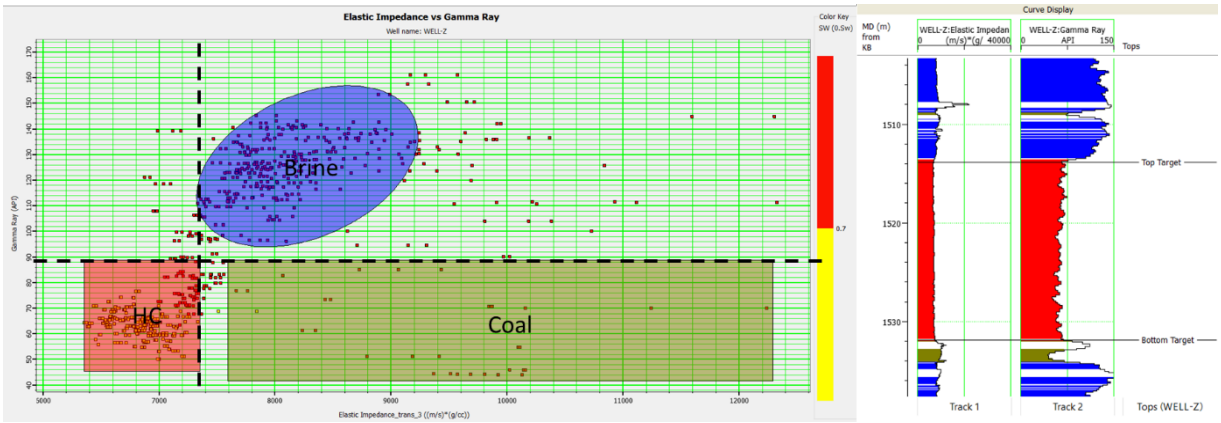

Gambar 6. *Cross-plot of EEI 38º and Gamma-ray logs, with SW color key*

EEIPre-Inversion Analysis

Before the inversion analysis is carried out, an initial (initial) model is made which is used to estimate the shape of the subsurface. To create an initial inversion model, seismic data and log data are needed which consist of: s-wave, p-wave, density, and elastic impedance. In making the initial model of this inversion, a frequency highcut of 10/15 Hz was used. The resulting initial model has a similar structural form as shown in seismic data, where the anticline structure is very visible in the Z-Well area.

After obtaining the initial inversion model, an inversion analysis can be carried out to find out the model and the right parameters for the inversion process. In this inversion analysis, experiments were carried out with various models and parameters, as shown in Table 2. Based on Table 3 it can be seen that the model that produces the best correlation, and the smallest error, is an inversion with the Based model, with Hard Constraints. Based on the Hard Constraint Based model, a very good correlation value is obtained, which is at 0.997, with an error value of 0.078.

Journal of Earth Energy Engineering
Vol. 12 No. 2s 2023: IC-UPERTAIN 2022, pp 1-10

Table 2. Inversion Model Correlation

No	Method	Correlation	Error
1	Model-Based Hard Constraint	0.995	0.093
2	Model-Based Soft Constraint	0.967	0.256
3	Bandlimited	0.893	-
4	Colored Inversion	0.815	-
5	Linear Programming Spare Spike	0.952	0.306

Figure 7 can be seen for the qualitative analysis of the inverse correlation with the model based on the EI log (elastic impedance) for the inverted and the original log. It can be seen that the deflection curve on the inverted log is similar to the original log, and the original and synthetic seismic traces also show similarities in the amplitude pattern. Based on the quantitative analysis, it can be seen that the correlation obtained is very good, namely 0.993 and an error value of 0.093 (Figure 9).

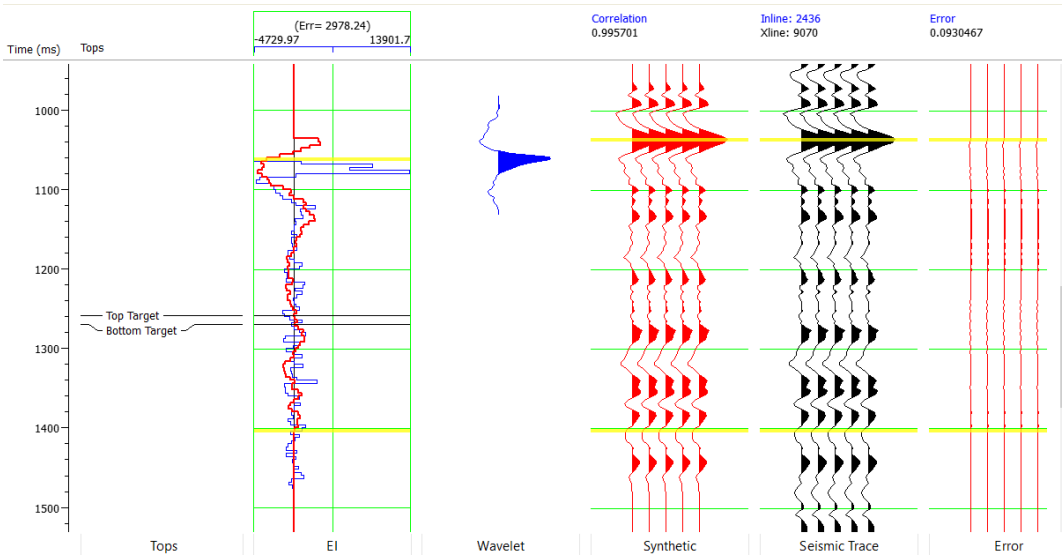

Figure 7. Post-Stack Inversion Model-Based Soft Constraint Analysis

EEI Inversion Result Analysis

After the inversion analysis was carried out, the best model and parameters were obtained, namely the Based model with Hard Constraints. The results of the inversion with the Based model can be seen in Figure 8. In Figure 8 you can see the results of the inversion of the target zone in the Z-field, where you can see the pattern of reservoir distribution around the Z-well. The reservoir zone in the target zone at a depth of 1258 ms - 1269 ms has an EEI value in the moderate range, which is at 6000(m/s)(g/cc) - 7500(m/s)(g/cc), which is indicated by a red anomaly in the inversion section (Figure 4.12). This target zone is estimated to be composed of sandstones, originating from the Balikpapan Formation in the study area which was formed in the Middle Miocene-Late Miocene. The results of this inversion also show the cap rock zone which is composed of shale (shale) and it is also suspected that coal is deposited. The shale (shale) and coal zones have higher EEI values than the sandstone zones, but the shale (shale) and coal zones have almost similar EEI values, and they overlap. The shale zone (shale) is scattered in alternating sandstones as cap rock, in the EEI range of 7500(m/s)(g/cc) - 9200(m/s)(g/cc). The shale zone (shale) is shown by the light blue to dark blue EEI anomaly in the inversion model. There is quite a lot of coal in this Z-field which intersects the sandstones in this formation. The distribution of coal in the Z-well area is thought to be spread over the EEI range of 7500(m/s)(g/cc) - 12000 (m/s)(g/cc) which is marked by light blue to purple anomalies in the Z-well area. The presence of coal in the Z-well of the Z-field is thought to have originated from the Balikpapan Formation in the Z-field.

Copyright @ Haq et al; This work is licensed under a Creative Commons Attribution-ShareAlike 4.0 International License.

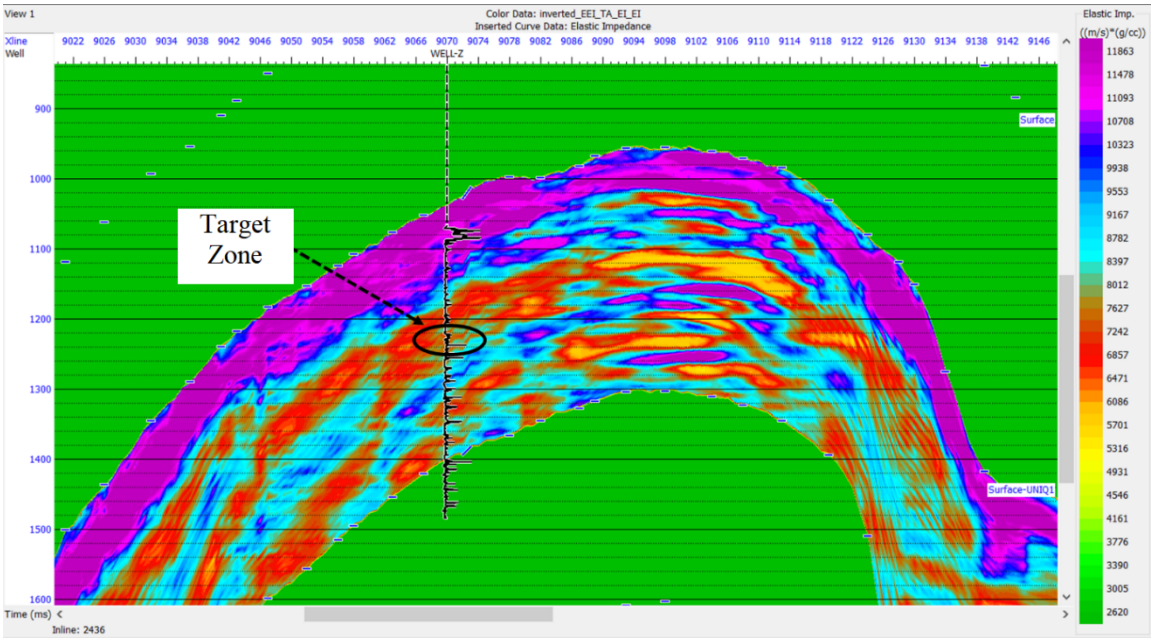

Figure 8. Inversion Result Model

Figure 9 is the result of Slicing performed on the EEI inversion results. Based on the Slicing map in Figure 9, it can be seen that the EEI distribution pattern for sandstone reservoirs in the Z-well research field is in the medium range EEI values, which are in the range of 6000 (m/s)(g/cc) -7500 (m/s))(g/cc). This target zone is estimated to be composed of sandstones, originating from the Balikpapan Formation in the study area. This sandstone zone is thought to spread around the field in a northeast-to-south direction, which is marked in yellow to orange. The shale (shale) and coal zones have higher EEI values than the sandstone zones, with nearly similar EEI values, and overlapping each other. Zones with high EEI values are indicated to be composed of shale (shale) as cap rock in the EEI 7500 (m/s)(g/cc) - 9200 (m/s)(g/cc) range, which is light blue to dark blue. located in the middle of the field towards the south. while the EEI value which is also high in the EEI range of 7500 (m/s)(g/cc) - 12000 (m/s)(g/cc) is suspected of the presence of coal. The sandstone reservoir zone is shown by the yellow distribution in the study field which is spread from north to south in the east of the field.

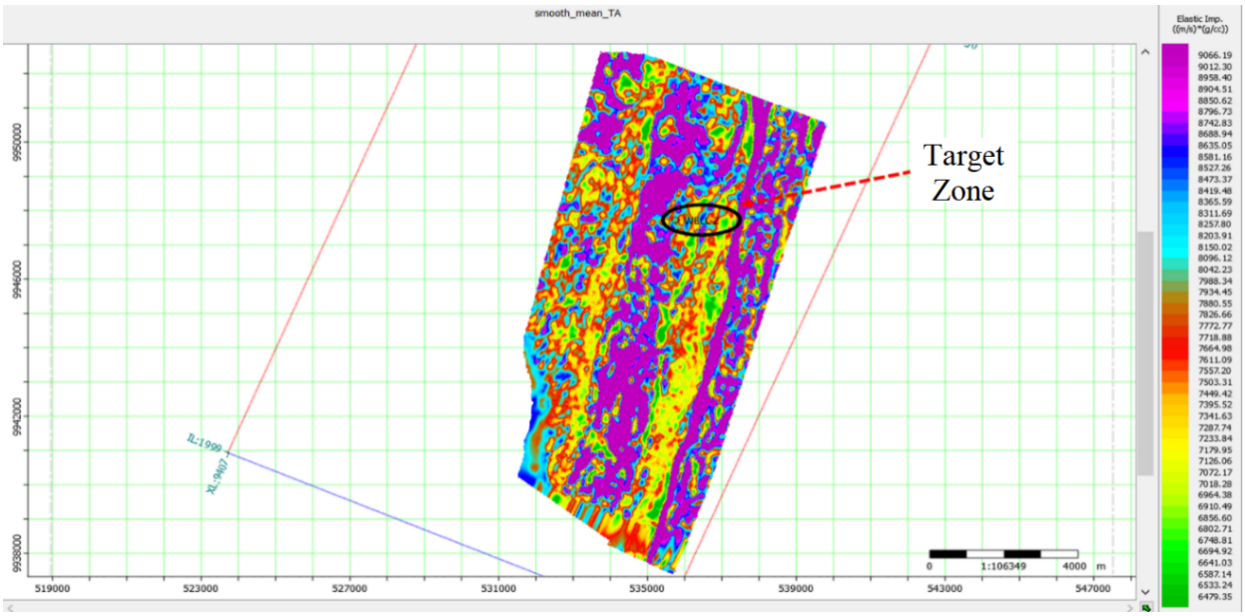

Figure 9. Slicing Inversion Model

Journal of Earth Energy Engineering
Vol. 12 No. 2s 2023: IC-UPERTAIN 2022, pp 1-10

CONCLUSION

Based on the analysis carried out, it can be concluded from this study that the EEI inversion uses the Based Hard Constraint model, with a Chi angle of 38 degrees. Based on the inversion results obtained, the sandstone reservoir in the Z field is in the EEI range of 6000 (m/s)(g/cc) - 7500 (m/s)(g/cc) spreading from northeast to south. The distribution of the sandstone reservoir is surrounded by coal with an EEI range of 7500(m/s)(g/cc) - 12000 (m/s)(g/cc), and also the distribution of shales in the EEI range of 7500(m/s)(g/cc) - 9200(m/s)(g/cc).

Acknowledgements

The authors extend their heartfelt appreciation to Mr. Aji Arif Sulaksono for their invaluable mentorship during the course of this research endeavor.

References

Ali, A.S., Othman, A.A.A., Ali, M.F. & Metwally, F. (2021). Extended Elastic Impedance Inversion for Better Delineation of Gas-bearing Sand Reservoir, Saffron Gas Field, Offshore Nile Delta, Egypt. *Austin Journal of Earth Science, 4*(1), 1023. https://doi.org/10.26420/austinjearthsci.2021.1023

Alam, H., Paterson, D. W., Syarifuddin, N., Busono, I., & Corbin, S. G. (1999). Reservoir potential of carbonate rocks in the Kutai Basin region, East Kalimantan, Indonesia. *Journal of Asian Earth Sciences, 17*(1–2), 203–214. https://doi.org/10.1016/S0743-9547(98)00047-6

Alebouyeh, M., & Chehrazi, A. (2018). Application of extended elastic impedance (EEI) inversion to reservoir from non-reservoir discrimination of Ghar reservoir in one Iranian oil field within Persian Gulf. *Journal of Geophysics and Engineering, 15*(4), 1204–1213. https://doi.org/10.1088/1742-2140/aaac50

Connolly, P. (1999). Elastic impedance. *The leading edge, 18*(4), 438-452. https://doi.org/10.1190/1.14383075

Hicks, G.J., & Francis, A.M. (2006). Extended elastic impedance and its relation to AVO crossplotting and Vp/Vs. In 68th EAGE Conference and Exhibition incorporating SPE EUROPEC 2006 (pp. cp-2). *European Association of Geoscientists & Engineers*. https://doi.org/10.3997/2214-4609.201402386

McClay, K., Dooley, T., Ferguson, A., & Poblet, J. (2000). Tectonic evolution of the Sanga Sanga Block, Mahakam Delta, Kalimantan, Indonesia. *AAPG Bulletin, 84*(6), 765–786. https://doi.org/10.1306/a96733ec-1738-11d7-8645000102c1865d

Moss, S. J. (2018). *Depositional modeling and facies architecture of rift and inversion episodes in the Kutai basin, Kalimantan, Indonesia*. https://doi.org/10.29118/ipa.1918.g.188

Moss, S.J., & Chambers, J.L. (1999). Tertiary facies architecture in the Kutai basin, Kalimantan, Indonesia. *Journal of Asian Earth Sciences, 17*(1-2), pp.157-181. https://doi.org/10.1016/S0743-9547(98)00035-X

Nugrahanto, K., Syafri, I., & Muljana, B. (2021). Depositional Environment of Deep-Water Fan Facies: A Case Study of the Middle Miocene Interval at the Kutei and North Makassar Basins. *Jurnal Geologi Dan Sumberdaya Mineral, 22*(1), 45. https://doi.org/10.33332/jgsm.geologi.v22i1.574

Pranata, G. D., Rosid, M. S., & Martian, D. (2017). Optimization of distribution and characterization of batupasir reservoir by using extended elastic impedance method in "g" old field. *AIP Conference Proceedings, 1862*(October). https://doi.org/10.1063/1.4991294

Purnomo, E.W., Abdul Latiff, A.H., & Elsaadany, M.M.A.A. (2023). Predicting Reservoir Petrophysical Geobodies from Seismic Data Using Enhanced Extended Elastic Impedance Inversion. *Applied Sciences, 13*(8), p.4755. https://doi.org/10.3390/app13084755

Satyana, A.H., Nugroho, D., & Surantoko, I. (1999). Tectonic controls on the hydrocarbon habitats of the Barito, Kutei, and Tarakan Basins, Eastern Kalimantan, Indonesia: major dissimilarities in adjoining basins. *Journal of Asian Earth Sciences, 17*(1-2), 99-122. https://doi.org/10.1016/S0743-9547(98)00059-2

Sun, Y-C., Chen, S-W., Li, Y-F., Zhang, J., & Gong, F-H. (2021). Shale (serpih) rocks brittleness index prediction method using extended elastic impedance inversion. *Journal of Applied Geophysics, 188*, 104314. https://doi.org/10.1016/j.jappgeo.2021.104314

Copyright @ Haq et al; This work is licensed under a Creative Commons Attribution-ShareAlike 4.0 International License.

Veeken, P.C.H., & da Silva, A.M. (2004). Seismic inversion methods and some of their constraints. *First break, 22*(6). https://doi.org/10.3997/1365-2397.2004011

Whitcombe, D. N. (2002). Elastic impedance normalization. *Geophysics, 67*(1), 60–62. https://doi.org/10.1190/1.1451331